

Identification of SPLUNC1's ENaC-Inhibitory Domain Yields Novel Strategies to Treat Sodium Hyperabsorption in Cystic Fibrosis Airway Epithelial Cultures

Carey A. Hobbs¹, Maxime G. Blanchard², Omar Alijevic², Chong Da Tan¹, Stephan Kellenberger², Sompop Bencharit³, Rui Cao¹, Mehmet Kesimer¹, William G. Walton⁴, Ashley G. Henderson¹, Matthew R. Redinbo⁴, M. Jackson Stutts¹ and Robert Tarran¹

¹Cystic Fibrosis/Pulmonary Research and Treatment Center, ³Department of Prosthodontics, ⁴Department of Chemistry, University of North Carolina, Chapel Hill, NC 27599
²Department of Pharmacology and Toxicology, University of Lausanne, Switzerland, CH-1005.

Running title: A SPLUNC1 peptide inhibits ENaC in CF airways

Please address correspondence to: Robert Tarran, Cystic Fibrosis/Pulmonary Research and Treatment Center, 7125 Thurston Bowles Building, UNC, Chapel Hill, NC 27599-7248.
Tel.: (919)966-7052; Fax: (919)966-5178; E-mail: robert_tarran@med.unc.edu

This research was published in the American Journal of Physiology – Lung cellular and molecular physiology. Hobbs, C. A., Blanchard, M. G., Alijevic, O., Tan, C. D., Kellenberger, S., Bencharit, S., Cao, R., Kesimer, M., Walton, W. G., Henderson, A. G., Redinbo, M. R., Stutts, M. J., and Tarran, R. (2013) Identification of the SPLUNC1 ENaC-inhibitory domain yields novel strategies to treat sodium hyperabsorption in cystic fibrosis airway epithelial cultures. Am J Physiol Lung Cell Mol Physiol 305, L990-L1001, doi: 10.1152/ajplung.00103.2013

ABSTRACT

The epithelial sodium channel (ENaC) is responsible for Na^+ and fluid absorption across colon, kidney and airway epithelia. Short Palate Lung and Nasal Epithelial Clone 1 (SPLUNC1) is a secreted, innate defense protein and an autocrine inhibitor of ENaC that is highly expressed in airway epithelia. While SPLUNC1 has a bactericidal permeability-increasing protein (BPI)-type structure, its N-terminal region lacks structure. Here we found that an eighteen amino acid peptide, S18, which corresponded to residues G22-A39 of SPLUNC1's N-terminus inhibited ENaC activity to a similar degree as full-length SPLUNC1 (~2.5 fold), whilst SPLUNC1 protein lacking this region was without effect. S18 did not inhibit the structurally related acid-sensing ion channels, indicating specificity for ENaC. However, S18 preferentially bound to the β -ENaC subunit in a glycosylation dependent manner. ENaC hyperactivity is contributory to cystic fibrosis (CF) lung disease. Unlike control, CF human bronchial epithelial cultures (HBECs) where airway surface liquid height (ASL) was abnormally low ($4.2 \pm 0.6 \mu\text{m}$), addition of S18 prevented ENaC-led ASL hyperabsorption and maintained CF ASL height at $7.9 \pm 0.6 \mu\text{m}$, even in the presence of neutrophil elastase, which is comparable to heights seen in normal HBECs. Our data also indicate that the ENaC inhibitory domain of SPLUNC1 may be cleaved away from the main molecule by neutrophil elastase, suggesting that it may still be active during inflammation or neutrophilia. Furthermore, the robust inhibition of ENaC by the S18 peptide suggests that this peptide may be suitable for treating CF lung disease.

Introduction

The epithelial sodium channel (ENaC) is the apical conduit for Na^+ absorption across a wide range of epithelia including renal, gastrointestinal and airway (22). The airway surface liquid (ASL) is composed of a mucus layer, which is responsible for trapping both inhaled particles and pathogens such as bacteria and a periciliary layer which facilitates ciliary beating and serves as a cell surface lubricant (32, 36). Airway epithelia can both absorb Na^+ through ENaC and secrete Cl^- through the cystic fibrosis transmembrane conductance regulator (CFTR). A precise balance of Cl^- secretion and Na^+ absorption across the airway is critical for regulating ASL volume. Normal human bronchial epithelial cultures (HBECs) regulate ASL height to an optimal depth of $\sim 7 \mu\text{m}$ while cystic fibrosis (CF) HBECs consistently show a much lower depth of $\sim 4 \mu\text{m}$ (32). ENaC is negatively regulated by CFTR (44) and in CF patients, CFTR's absence results in ENaC hyperactivity, leading to uncontrolled absorption of Na^+ and ASL volume depletion which slows or abolishes mucus transport. This lack of mucus transport leads to a failure to physically clear the lungs of accumulated mucus and inhaled pathogens and causes chronic lung infections which eventually leads to their destruction (40).

ENaC is made up of three subunits, α , β , and γ , which share $\sim 30\%$ sequence homology (12). Structurally, each subunit is made up of two transmembrane domains, short N- and C-terminal cytoplasmic tails and a large extracellular loop which contains numerous sites for N-linked glycosylation (11, 37). Activation of this channel occurs through proteolytic cleavage of the extracellular loops of the α and γ ENaC subunits by furin-type convertases (14, 25), membrane bound channel activating proteases (CAPs), such as prostasin (CAP1) and TMPRSS4 (CAP2) and/or soluble proteases including the serine proteases trypsin and neutrophil elastase (39). When these proteases are blocked by specific protease inhibitors, such as aprotinin for

trypsin-like proteases, ENaC activation is attenuated (8). Alternatively, the cleaved segments of α and γ ENaC may bind back into the channel and serve as inhibitory peptides (9, 13). Little is known about the physiological regulation of these key ENaC proteolytic processes. However, we recently hypothesized that a soluble modulator of ENaC existed in the ASL and designed a proteomic screen to identify it (20, 46). Our data indicated that the short palate, lung and nasal epithelial clone 1 (SPLUNC1) was the soluble modulator of both ENaC activity and ASL volume and knockdown of SPLUNC1 abolished ENaC regulation in normal HBECs, leading to CF-like ASL volume depletion (20). SPLUNC1 is endogenously secreted into the ASL and functions as an ASL volume sensor: as ASL volume increases, SPLUNC1 becomes diluted, removing the inhibition of ENaC and signaling for absorption to begin; conversely, when ASL volume is low, SPLUNC1 is concentrated, causing less ENaC activity.

SPLUNC1 is a 256 amino acid protein that belongs to the bactericidal permeability-increasing (BPI)-fold containing family A and is also known as BPIFA1, LUNX, PLUNC and SPURT. SPLUNC1 is expressed in the upper airways and nasopharyngeal regions and may also be expressed in Na^+ absorbing tissues including the colon and kidney (20). Based on sequence similarity with BPI-like proteins, SPLUNC1 was hypothesized to be an innate defense protein and indeed, SPLUNC1 has been shown to be both antimicrobial and to reduce surface tension (3, 15, 19, 49). More recently, SPLUNC1 has been proposed to be a multi-functional defense protein since its knockdown *in vivo* has been shown to decrease mucus clearance (33) as well as to increase *Mycoplasma pneumoniae* infection (19). Due to the wide variety of functions assigned to SPLUNC1, we set out to identify its ENaC inhibitory domain to better understand how this protein functions and how it interacts with ENaC.

EXPERIMENTAL PROCEDURES

Oocyte studies. *Xenopus laevis* oocytes were harvested and injected as previously described (18). Oocytes were studied 24 h post-injection using the 2 electrode voltage clamp technique as previously described (20). Where appropriate, oocytes were incubated with S18 or a control peptide, ADG, (described below) for 1 h prior to recording. ENaC activity was determined by measuring the amiloride-sensitive current. In some experiments β -ENaC^{S518C} was used, which forms ENaCs that are locked into a fully open state with an open probability near 1.0 by exposure to the sulphydral reactive reagent, [2-(Trimethylammonium)ethyl]methanethiosulphonate bromide (MTSET). MTSET was added at a concentration of 1 mM to the oocyte bath as previously described (43). Oocyte buffer solutions were used exactly as described previously (20).

Peptides. Peptides were synthesized and purified by the UNC Microprotein Sequencing and Peptide Synthesis Facility. The sequence of the S18 peptide was: GGLPVPLDQTLPLNVNPA. A control peptide of S18, ADG, was made by alphabetizing the sequence. The sequence of ADG was: ADGGLLLLNNPPPPPQTVV. Both peptides were used with either a free or biotinylated N- terminus as needed. Biotinylation had no effect on S18's ability to inhibit ENaC (n=6).

Electrophysiological measurements of ASICs. Previously described cell lines expressing human ASIC1a, human ASIC2a and rat ASIC3 were used in these experiments (34). Electrophysiological measurements were carried out with an EPC10 patch-clamp amplifier (HEKA Electronics, Lambrecht, Germany) as previously described (6).

Cell culture. HEK293T cells were cultured in DMEM/F12 medium containing 10% FBS, 1x penicillin/streptomycin, 0.2 µg/mL puromycin, and 0.1 mM hygromycin at 37°C/5% CO₂ on 6-well plastic plates. Cells were transfected according to the manufacturer's instructions using Lipofectamine 2000 (Invitrogen, Carlsbad, CA, USA) using the DMEM/F12 media. Cells were transfected when 90-95% confluent with 0.5 µg of plasmid DNA per construct per well and incubated at 37°C/5% CO₂ overnight. CHO cell lines stably expressing human ASIC1a, human ASIC2a and rat ASIC3 were used in the electrophysiological measurements of ASICs (34).

Human excess donor lungs and excised recipient lungs were obtained at the time of lung transplantation and cells were harvested by enzymatic digestion as previously described under a protocol approved by the UNC Institutional Review Board (46). HBECs were maintained at an air-liquid interface in a modified bronchial epithelial growth medium (BEGM) with 5% CO₂ at 37°C and used 2-5 weeks after seeding on 12-mm T-clear inserts (Corning-Costar, Corning, NY, USA) (35). For experiments performed out of the incubator, both HEK293T cells and HBECs were maintained in a modified Ringer solution as described previously (20).

Peptide pull-down assay and western blotting. HEK293T cells were plated in standard plastic 6 well plates (Corning Costar) transfected with double-tagged human ENaC subunits with HA and V5 epitopes at the N- and C- termini, respectively, in combination with wild-type untagged subunit cDNA when 90% confluent. When all three ENaC subunits were expressed, 0.5 µg of each subunit were transfected. When expressed individually, 0.75 µg of the subunit was transfected. The transfected cells were lysed 24 h later using NP-40 buffer with 1x complete EDTA-free protease inhibitor (Roche, Basel, Switzerland). The lysate was centrifuged at 16,300 x g for 15 min at 4°C and the supernatant collected. Protein concentration was determined using

the BCA assay and 500 µg of protein plus 0.25 mg peptide and 100 µL of neutravidin were added to a spin column and rotated end-over-end at 4°C for 24 h (all ThermoFisher Scientific, Rockford, IL, USA). Flow-through was collected by centrifugation at 1000 x g for 30 s. The beads were then washed 5 times with NP-40 buffer. Bound protein was eluted by boiling at 95°C for 10 minutes in 75 µL of 2 times LDS NuPAGE sample buffer with 1x sample reducing agent followed by centrifugation at 16,300 times g for 2 min. Samples were resolved on 4-12% Bis-Tris gels in MES and transferred to a nitrocellulose membrane using iBlot, setting P3 for 8 min (Invitrogen, Carlsbad, CA, USA). The membrane was probed using 1:1000 anti-V5 antibody (Invitrogen, Carlsbad, CA, USA) overnight at 4°C in 3% fish gelatin in TBS-T. The blot was then incubated for 1 h at room temperature with an ECL sheep anti-mouse IgG secondary antibody and detected by ECL reagent (ThermoFisher Scientific, Waltham, MA, USA) or by incubation with a goat anti-mouse IRDye secondary antibody and analyzed by an Odyssey infrared imaging system (LI-COR Biosciences, Lincoln, NE, USA). Pull-down was performed using an N-terminally biotinylated version of S18 or ADG. Biotinylation had no effect on the ability of S18 to inhibit ENaC (n=12).

Deglycosylation. Peptide pull-down assays were performed as described above. Samples were eluted by the addition of 100 µL of 0.1 M sodium citrate, pH 5.5, 0.1% SDS to the beads and incubating at 100°C for 2 min, followed by centrifugation at 16,300 x g for 2 minutes. The samples were divided equally, and one half was treated with 1 µL of EndoH and incubated at 37°C for 2 min. After incubation, all samples were lyophilized and then reconstituted in 30 µL LDS NuPAGE sample buffer with 1x sample reducing agent (Invitrogen, Carlsbad, CA, USA). Western blots were completed as described above. A concentration of 5 µg/ml tunicamycin (Sigma-Aldrich, St Louis, MO, USA) was added to the cell transfection media and the cells were

incubated overnight at 37°C/5% CO₂. The following day the protocol for the peptide pull-down assay was performed as described above.

ASL height measurements. To label the ASL, 20 µl PBS containing 10 kDa Rhodamine dextran (0.2-2 mg/mL; Invitrogen, Carlsbad, CA, USA) was added to HBEC mucosal surfaces as previously described (45). When added, peptides with or without 100 nM neutrophil elastase, 1 U/mL aprotinin, activated neutrophil supernatant (ANS) (23) or 10 µM sivelestat (Sigma-Aldrich, St Louis, MO, USA) were added to the mucosal surface along with the Rhodamine dextran. In some cases, bumetanide (100 µM) was added to the serosal solutions for the duration of the experiment. The HBEC mucosal surfaces were washed with 500 µL PBS for 30 min prior to experimentation to remove accumulated endogenous SPLUNC1. SPLUNC1 recovery into the ASL was measured over time by lavaging with 200 µL PBS at timed intervals after the initial wash/volume load. To detect SPLUNC1, 20% by volume of the lavage was transferred onto a nitrocellulose membrane using a slot blot apparatus (GE Healthcare, USA). The blot was processed as described above using an anti-hPLUNC primary antibody (R & D Systems, Minneapolis, MN, USA).

Transepithelial potential difference (V_t) studies. A single-barreled V_t -sensing electrode was positioned in the ASL by micromanipulator and used in conjunction with a macroelectrode in the serosal solution to measure V_t using a voltmeter (World Precision Instruments, Sarasota, FL, USA) as described (20). Bumetanide (100 µM) was present for all measurements to inhibit V_t due to Cl⁻ secretion. To calculate the amiloride-sensitive V_t , V_t was measured, amiloride was added as a dry powder in perfluorocarbon and V_t was remeasured 10 min later. Thus, the amiloride-sensitive V_t constitutes the difference between these values.

Circular dichroism (CD). 100 µM S18 was dissolved in a buffer containing 10 mM sodium phosphate, pH 7.4 in a 1 mm cuvette. Using a Chirascan-plus instrument (Applied Photophysics Limited, Leatherhead, UK), five individual spectra from 185 to 280 nm were recorded at 25 ± 1.0°C and averaged. All measurements were corrected for buffer signal.

Expression and Purification of Human SPLUNC1. Full-length SPLUNC1 cDNA was kindly provided by Dr. Colin Bingle. The SPLUNC1-Δ19 and Δ44 constructs were created by cloning amino acid residues 20–256 or 45-256 out of the SPLUNC1 cDNA for entry into pMCSG7 for protein expression. BL21-CodonPlus competent cells (Agilent Technologies, Santa Clara, CA, USA) were transformed with the expression plasmid and cultured in the presence of antifoam (50 µL), ampicillin (100 µg/mL) and chloramphenicol (34 µg/mL) in LB medium with vigorous shaking at 37°C until an OD₆₀₀ of 0.6 was attained. Expression was induced with the addition of isopropyl-1-thio-D-galactopyranoside (IPTG). Bacteria were collected by centrifugation at 4500 x g for 20 min at 4°C. Cell pellets were resuspended in Buffer A (20 mM Potassium Phosphate, pH 7.4, 50 mM Imidazole, 500 mM NaCl and 0.02% NaAzide) along with lysozyme, DNase1, and protease inhibitor tablets. Cells were sonicated and cell lysate was separated into soluble and insoluble fractions using high-speed centrifugation. The soluble fraction was filtered then flowed over a Ni-NTA His-Trap gravity column and washed with Buffer A. The bound protein was eluted with Buffer B (20 mM Potassium Phosphate, pH 7.4, 500 mM Imidazole, 500 mM NaCl and 0.02% NaAzide) and separated using an S200 gel filtration column on an ÄKTAXpress™. The C-terminal histidine tag was removed with Tev protease as described before experimentation (21). Another round of nickel and HPLC purification removed the tag from the purified SPLUNC1-Δ19. We confirmed that SPLUNC1-Δ19 purified in this fashion inhibited ENaC in CF airways (n=6).

Neutrophil elastase cleavage of SPLUNC1-Δ19 and analysis by LC-ESI/MS/MS.

Neutrophil elastase was added to SPLUNC1-Δ19 at a ratio of 1:1000 (enzyme: protein) followed by incubation for 5, 15 and 60 min at 37°C. Digested samples (5 µL) were introduced to a Q-Tof *micro* mass spectrometer (Waters, Manchester, UK) via a nano-acquity UPLC (Waters, Milford MA, USA) system as described previously (31). Briefly, the analytical system was configured with a PepMap™ C18 (LC Packing, 300µm ID x 5mm) pre-concentration column in series with an Atlantis® (Waters) dC18 NanoEase™ (75 m x 150 mm) nanoscale analytical column. Peptides were separated on the column with a gradient of 5% acetonitrile in 0.1% formic acid to 60 % acetonitrile in 0.1% formic acid over 60 min and were directly analyzed without addition trypsin digestion. All data were acquired using MassLynx 4.1 software. The raw data acquired were processed using the ProteinLynx module of MassLynx 4.1 to produce *.pkl (peaklist) files which are suitable for the MS/MS ions database search via search engines. The data processed was searched against the Uniprot protein database (release 2011_09) using an in house MASCOT (Matrix Science, London, UK) search engine (Version 2.2). MASCOT probability based Mowse individual ion scores > 40 were accepted as indicating identity or extensive homology ($p<0.05$).

SPLUNC1 peptides in CF patients and donor sputum. Human sputum samples were obtained as previously described (30). The study protocol was approved by the University of North Carolina Committee on the Protection of Rights of Human Subjects, and informed consent was obtained. Sputum from 4 CF patients and 4 healthy donors were pooled, respectively. 1 mL of pooled sputum from each group was diluted in 4 mL PBS. The samples were filtered through a 0.22 µm membrane (Millipore, Bedford, MA). The resulting filtrate were injected onto an Ettan LC chromatographic system (Amersham Pharmacia Biotech, Piscataway, NJ) with a Superdex 200 HR 10/30 chromatography column. The large proteins were separated from the

low-molecular-weight peptides with PBS elution at a flow rate of 0.3 mL/min. The peptide pool was dried down 10x by volume using a vacuum concentrator and then mixed 1:1 with 1% formic acid and subjected to nano-LC-electrospray ionization-tandem MS (MS/MS) and analyzed using the above parameters. N.B., unlike conventional proteomic studies, the sputum samples were not trypsin-digested and only peptides that were endogenously formed were detected while all other protein was excluded from the analysis.

Statistical analyses. Unless otherwise noted, all data are presented as means \pm se for n experiments. Differences between means were tested for statistical significance using paired or unpaired t tests when the variances were homogeneously distributed, or in the case of nonhomogeneity of variance, the Wilcoxon rank-sum or Mann-Whitney U tests were used as appropriate. From such comparisons, differences yielding values of $P \leq 0.05$ were judged to be significant. HBECs derived from ≥ 3 donors were used per experiment, and experiments using cell lines were repeated on 3 separate occasions. All analyses were conducted using Instat software (GraphPad, San Diego, CA, USA).

RESULTS

Identification of SPLUNC1's ENaC inhibitory domain.

SPLUNC1 is a 256 amino acid protein that has a cleavable N-terminal signal sequence. We have recently resolved the crystal structure of SPLUNC1 lacking this signal sequence ($\Delta 19$ -SPLUNC1) (21). Interestingly, the N-terminal region up to residue 43 was different from the rest of SPLUNC1 in that it lacked any discernible structure. However, a peptide, termed S18, which corresponded to this unstructured N-terminal region of SPLUNC1 (²²GGLPVPLDQTLPLNVNPA³⁹), prevented cleavage of γ ENaC in HBECs derived from both normal and CF subjects (21). To examine the effects of S18 on HBECs in more detail, we first

examined its onset of action. Inhibition of ENaC can cause hyperpolarization of the apical membrane and increase the transepithelial voltage (V_t) caused by Cl^- secretion (24). Thus, we exposed HBECs to serosal bumetanide to inhibit Cl^- secretion before measuring V_t , since under these conditions, the remainder of V_t is largely due to ENaC activity/ Na^+ absorption (Fig. 1A). The S18 peptide significantly inhibited the bumetanide-insensitive V_t in normal HBECs in a similar time as SPLUNC1 $^{\Delta 19}$, whilst an alphabetized version of S18 (ADG, control) was without effect. Furthermore, amiloride strongly inhibited V_t in ADG- and vehicle- treated but not S18- or SPLUNC1-treated cultures. When added mucosally for 1 h, both S18 and SPLUNC1 $^{\Delta 19}$ both inhibited the amiloride-sensitive V_t . In contrast, $\Delta 44$ -SPLUNC1, which lacks the S18 region (i.e. amino acids G22-A39) had no significant effect, suggesting that SPLUNC1's ENaC inhibitory domain was located at the N-terminus of SPLUNC1 (Figure 1B).

To confirm that S18 was acting on ENaC, we co-injected oocytes with α , β^{SS18C} , γ ENaC subunits and incubated them with 10 or 100 μM S18 for 1 h. We subsequently observed an ~ 2.5 fold decrease in I_{NA} ($p < 0.05$), indicating that we had identified the ENaC inhibitory domain of SPLUNC1 (Figure 2A). To further explore the effects of S18, MTSET was added during recording to lock the channel into a fully open position and give an approximation of the number of active channels in the plasma membrane (38, 43). MTSET significantly increased ENaC activity ~ 6 fold over basal current levels (Figure 2B). In the presence of S18, MTSET still raised I_{NA} above basal levels. However, the increase was significantly less than under control conditions, suggesting that exposure to S18 resulted in a decrease in surface ENaC levels (Figure 2B). In contrast, when incubated with the control peptide, ADG, no difference in the I_{NA} was observed (Figure 2C).

Structurally related acid-sensing ion channels (ASICs) are not inhibited by S18.

We tested whether SPLUNC1 affected the function of the related ENaC/degenerin family members, the acid-sensing ion channels (ASICs). In order to assess possible effects of S18 on the pH dependence of ASIC activation and on current amplitude, channels were activated by a change from pH 7.4 to a pH corresponding to the steep phase of their activation curve, pH 6.6 for ASIC1a and -3, and 4.0 for ASIC2a. At these stimulation pH values, a change in current expression or pH dependence would be readily detected as a change in the measured current amplitude. Stimulations of 5 s duration were performed every 45 s to allow recovery from inactivation between stimulations. Three control values were obtained before switching to a pH 7.4 solution containing 10 μ M S18. The S18 peptide was then present during 3 stimulation rounds in both the conditioning (pH 7.4) and the acidic stimulation solution before it was washed out. Figure 3A illustrates a typical experiment with an ASIC1a-expressing cell. Average current amplitudes were normalized to the first control value and plotted as a function of time (Figure 3B). The peptide had no apparent effect on the activation properties of the different ASICs tested ($n=3$ by channel type, $p>0.05$). No changes in current kinetics were observed (not shown). When exposed to a pH that is less than pH 7.4, but is insufficiently acidic to activate the channel, ASICs inactivate directly from the closed state. This process is known as steady-state inactivation (SSI). Its pH dependence has been determined to have a midpoint of pH 7.2 for ASIC1a, pH 7.1 for ASIC3 and 5.6 for ASIC2a (6). To detect changes in the pH dependence of SSI due to the presence of the peptide, cells were incubated 40 s in a conditioning solution with a pH close to the midpoint of SSI, in the presence or absence of the peptide (7.1 for ASIC1a, and -3, pH 5.6 for ASIC2a). The conditioning period was followed by activation with an acidic stimulus (pH 6.0 for ASIC1a and -3 and pH 4 for ASIC2a). Figure 3C plots the average values of the current after the conditioning period normalized to the maximal current obtained with a

conditioning pH of 7.4. The peptide does not modify the pH dependence of steady-state inactivation of the tested ASICs.

Cleavage of ASIC1a channels by trypsin leads to a shift in the pH dependence of activation to more acidic values (34). ASIC1a was first activated three times by pH 6.6, every 45 s. The conditioning solution was then switched to a pH 7.4 solution containing 40 µg/ml trypsin with or without 10 µM S18, and currents were measured every 45 s at pH 6.6. Due to the trypsin-elicited time-dependent shift in the pH dependence of activation, we observed a gradual reduction in pH 6.6-evoked current in the presence of trypsin, as illustrated in Figure 3D. This current decrease was not prevented by S18.

Since S18 takes up to one hour to fully inhibit ENaC (Figure 1A), we then pre-exposed ASICs to S18 for 1 h before performing patch clamp studies. This maneuver had no effect on ASIC1a or ASIC3 current densities (Figure 4). However, ASIC2a was significantly activated by this 1 h pretreatment (Figure 4).

S18 may interact through the β-ENaC subunit.

Using co-immunoprecipitation, we have previously demonstrated that SPLUNC1 binds to αβγ-ENaC (20). A pull-down assay was performed using biotin-labeled S18 to determine if the peptide was also able to interact with ENaC in a similar fashion. Three different transfections were performed with one of the three subunits V5-tagged and the other two untagged. The cell lysates were then incubated with biotinylated S18 bound to neutravidin beads. As observed with full-length SPLUNC1, S18 was found to pull-down all three ENaC subunits, although βENaC was more strongly pulled down than either α- or γ- ENaC (Figure 5A). To further characterize this interaction, each subunit was expressed individually and the pull-down assay repeated. In this case, only β-ENaC was detected in the elution, suggesting that under these conditions, S18

binds exclusively to the β -ENaC subunit and not to the α - or γ - subunits (Figure 5B). When the pull-down assay of the β -ENaC subunit was performed with ADG, β -ENaC was not detected in the elution, confirming that S18 is specifically binding to the β -ENaC subunit (Figure 5C).

β -ENaC glycosylation is required for the β -ENaC/S18 interaction.

The predicted molecular weight of a non-glycosylated β -ENaC subunit is ~73 kDa. However, the extracellular loop of β -ENaC contains 12 possible sites for *N*-linked glycosylation and β -ENaC is typically observed at 94-96 kDa due to extensive *N*-linked glycosylation (25). As seen in Figure 5, the molecular weight of the β -ENaC subunit which predominantly interacted with the S18 peptide was around 94 kDa. To confirm that this was glycosylated β -ENaC, the elution of the $S18/\alpha,\beta^{V5},\gamma$ ENaC pull-downs were deglycosylated with Endoglycosidase H (EndoH) (Figure 6A). As previously described (25), upon treatment with EndoH, the 94 kDa β -ENaC band shifted to ~73 kDa, consistent with the deglycosylation of β -ENaC (Figure 6A). This experiment was repeated with the β^{V5} -ENaC subunit expressed alone. Upon EndoH treatment, this band shifted to ~73 kDa (Figure 6B). EndoH treatment could only be performed once the pull-down assay had been completed; therefore, to test whether S18 was able to interact with non-glycosylated β -ENaC, we exposed cells expressing either α,β^{V5},γ ENaC or β^{V5} ENaC to tunicamycin, an inhibitor of *N*-linked glycosylation (48). The pull-down assay was then performed on the tunicamycin-treated cell lysate (Figures 6C, D). As seen in the input lanes, treatment with tunicamycin reduced the molecular weight of the β -ENaC subunit to ~73 kDa, confirming that the protein was deglycosylated. No β -ENaC was observed in the elution of the tunicamycin treated pull-downs (Figures 6C, D). Combined with the EndoH data, these data indicate that S18 is interacting with a specific, glycosylated form of β -ENaC.

S18 attenuates ASL hyperabsorption in CF HBECs through ENaC inhibition.

To determine if S18 was capable of inhibiting ENaC dependent ASL absorption in native airway epithelia, we measured ASL height over time in both normal and CF HBECs after treatment with S18 (Figure 7A, B). SPLUNC1 is endogenously secreted by both normal and CF HBECs, which could affect ASL volume regulation, especially in normal HBECs (20). Thus, we standardized the mucosal washing/volume-loading protocol accordingly so that every culture had endogenous SPLUNC removed prior to t=0. Each culture was left with undisturbed ASL for 24 h. They were then incubated for 30 min with 500 μ L PBS followed by two quick successive washes with 500 μ L PBS. Then, 20 μ L of PBS containing rhodamine-dextran was added as a volume challenge with or without peptide. Slot-blot analysis revealed that it took 24 h for SPLUNC1 levels in the ASL to recover to baseline values (Figure 7B, inset). Vehicle-treated CF HBECs had a significantly lower ASL height than normal controls. However, the ASL height in CF S18 treated samples, $7.9 \pm 0.6 \mu\text{m}$, was significantly higher than the CF controls, $4.2 \pm 0.6 \mu\text{m}$. This increase in ASL height in S18 exposed CF HBECs was comparable to that observed in normal HBECs ($\sim 8 \mu\text{m}$). Next, a full dose response was completed in order to calculate the IC₅₀ by measuring the ASL height of both normal and CF HBECs 6 h after addition of S18 (Figure 7C). The IC₅₀ was not significantly different between normal and CF HBECs, $0.29 \pm 0.19 \mu\text{M}$ and $0.52 \pm 0.23 \mu\text{M}$, respectively.

To test whether S18 specifically affected ENaC in normal and CF HBECs, the 24 h transepithelial potential difference (V_t) was measured (Figure 7D,E). In the normal HBECs, a basal V_t of $-6.6 \pm 0.5 \text{ mV}$ was observed and this decreased to $-10.6 \pm 0.7 \text{ mV}$ following a brief exposure to trypsin, which is indicative of ENaC activation (46). S18 had little additional effect on the 24 h V_t in normal HBECs. Consistent with our previous observation that CF ENaC remains fully active and non-responsive to trypsin (46), the CF vehicle-exposed HBECs had an

elevated V_t of -15.2 ± 0.9 mV and trypsin had no further effect. In contrast, after 24 h exposure to S18, the CF HBEC V_t was significantly lowered to -8.4 ± 0.9 mV, and a 30 min exposure to trypsin changed the V_t to -11 ± 0.7 mV, suggesting that S18 works through ENaC in CF HBECs. In contrast, ADG had no effect on normal or CF HBEC V_t (both $n=6$). To further confirm that S18 functions by inhibiting ENaC hyperabsorption, the ASL height of normal HBECs was measured over time in the presence of bumetanide with or without S18 (Figure 7F). Serosal bumetanide significantly decreased normal ASL height toward CF levels (i.e. <5 μm). In contrast S18 was able to maintain significantly greater ASL height even in the presence of bumetanide, indicating that S18 increases ASL height by inhibiting absorption not secretion.

S18 has no intrinsic structure.

To better understand how S18 may interact with ENaC, we next looked for intrinsic structure in this peptide. Since the S18 regions does not show up in the crystal structure of SPLUNC1 (21), we next used the program PSIPRED to predict its structure (10, 26). No structure was predicted with PSIPRED and we also failed to detect any secondary structure by circular dichroism (Figure 8A). To functionally test this hypothesis, we heat denatured S18 by incubating it at 67°C for 30 min, added it to the mucosal surface of CF HBECs and then measured ASL height 2 h later. The heat denatured S18 was able to prevent ASL hyperabsorption to the same extent as the non-heat denatured peptide (Figure 8B), suggesting that S18 performs its function with no intrinsic secondary structure.

S18 prevents CF ASL hyperabsorption in the presence of neutrophil elastase.

CF airways are characterized by chronic neutrophilia and display a significantly higher level of neutrophil elastase activity than normal airways (47). Since neutrophil elastase has

previously been shown to activate ENaC by cleaving the γ subunit (39), we tested whether S18 was still capable of inhibiting CF ASL hyperabsorption in the presence of this protease (Figure 9A). Mucosal addition of S18, but not ADG, to CF HBECs resulted in a significant increase in ASL height. Similarly, aprotinin which blocks trypsin-like proteases, was also able to maintain ASL height to a similar degree as S18. Interestingly, S18 maintained its ability to prevent CF ASL hyperabsorption in the presence of neutrophil elastase, while aprotinin was unable to prevent neutrophil elastase induced ASL height depletion. Activated neutrophil supernatant (ANS), which is derived from human neutrophils, contains high levels of neutrophil elastase activity (23), but did not diminish S18's ability to prevent CF ASL volume hyperabsorption. When the neutrophil elastase inhibitor sivelestat, also known as ONO-5046, was added to the ASL along with S18 and NE, no further effect on ASL height was observed (Figure 8B). Together these data suggest that S18 may be able to prevent ASL hyperabsorption, even in the presence of the high proteolytic activity that is typically present in diseased CF lungs.

Cleavage of SPLUNC1 by neutrophil elastase.

To determine whether peptides corresponding to the N-terminal ENaC inhibitory domain of SPLUNC1 may be released from the main molecule by neutrophil elastase, the SPLUNC1- Δ 19 recombinant protein which lacks the N-terminal signaling sequence but contains the ENaC inhibitory domain was exposed to neutrophil elastase for 5, 15 and 60 min and the resulting cleavage products determined by mass spectrometry. Similar sequence coverage was observed at all three time points ~80% (Figure 9C, Table 1). Three peptides were observed by mass spectrometry that spanned the ENaC inhibitory domain (i.e. residues 23-45) at all three time points: two ions corresponding to peptide $^{23}\text{GLPVPLDQLPLNVNPALPLSPT}^{45}$ with a *m/z* of 1183.74²⁺ and 789.49³⁺ were observed; two ions corresponding to peptide

²⁷PLDQTLPLNVNPALPLSPT⁴⁵ with a *m/z* of 1000.59²⁺ and 667.39³⁺ were observed and one ion corresponding to peptide ³²LPLNVNPALPLSPT⁴⁵ with a *m/z* of 723.41²⁺ was observed. In addition to this, in the 15 and 60 min samples one ion corresponding to peptide ²⁰QFGGLPVPLDQTLPL³⁴ with a *m/z* of 797.99²⁺ was observed. Several other peptides spanning this region were observed in the 60 min sample only including an ion corresponding to peptide ²³GLPVPLDQTLPLNVNPA³⁹ with a *m/z* of 879.53²⁺. All peptides observed in the 5 min sample are listed in Table 1.

Next, we determined which, if any, SPLUNC1 peptides were present in human sputum. In sputum obtained from normal subjects, four peptides were observed that spanned the ENaC inhibitory domain: an ion corresponding to peptide ²⁸LDQTLPLNVNPALPLSPT⁴⁵ with a *m/z* of 952.03²⁺, one ion corresponding to peptide ²⁹DQTLPLNVNPALPLSPT⁴⁵ with a *m/z* of 895.49+, one ion corresponding to peptide ³²LPLNVNPALPLSPT⁴⁵ with a *m/z* of 723.41²⁺ and one ion corresponding to peptide ³⁵NVNPALPLSPT⁴⁵ with a *m/z* of 561.81²⁺ were observed. Surprisingly, no peptides were observed in CF sputum before residue 46, consistent with our previous studying demonstrating that SPLUNC1's regulation of ENaC is defective in CF airways (21).

DISCUSSION

We have recently resolved SPLUNC1's structure to 2.8 Å (21). As expected, SPLUNC1 displays the a "half boomerang" shape that is typical of the bactericidal permeability-increasing protein/lipopolysaccharide-binding protein (BPI/LBP) superfamily (4). In contrast, the N-terminal domain (residues 20-43) had no observable structure. Surprisingly, we found that a peptide which reprised this unstructured region, S18 (Residues G22-A39), inhibited ENaC to the same extent as Δ 19-SPLUNC1, whilst SPLUNC1 lacking the S18 region (Δ 44-SPLUNC1) was without effect (Figure 1A, B). We have previously shown that SPLUNC1 lowers ENaC surface densities (38). Since S18 and SPLUNC1 act over a similar time-frame, it is possible that S18 also reduces plasma membrane ENaC levels, rather than acting as a rapid-onset, amiloride-like pore blocker.

In the presence of MTSET, S18 caused a significant decrease in ENaC activity. We have assumed the MTSET has its usual effect in our study, i.e., to increase ENaC P_o to \sim 1.0 (1). One can divide the MTSET current by the basal current to give estimate the degree of activation by MTSET. Due to the depression of basal currents, MTSET activation was significantly greater in the presence of S18 than in its absence (9 fold vs. 5.7 fold respectively). This ratio has previously been taken as an indicator of channel open probability (P_o) and the higher fold increase may indicate that ENaC resides in a lower P_o in the presence of S18 (Figure 2) (1). Therefore, while it is likely that S18 decreases N, we cannot exclude the possibility that S18 may also have an additional effect on P_o . Thus, an S18-induced reduction in MTSET-activated ENaC currents is consistent with S18 predominantly affecting N. However, absent single channel data, which is not available to us at present, the possibility that S18 also affects P_o still remains to be tested.

Despite being structurally related to ENaC, our experiments did not show any inhibitory effect of S18 on ASIC activity following either acute or 1 h exposure to this peptide (Figures 3, 4). In the absence of an endogenous regulation of ASICs by proteases in the cell system used (34), a long-term exposure to S18 was not expected to have an effect. However, we did find that the 1 h exposure to S18 significantly activated ASIC2a. ASICs are the target of peptide toxins and of short peptides and several small, charged peptides have been shown to acutely modulate ASIC function (2, 42). Currently there is no evidence of endogenous regulation of ASICs by proteases, although it is known that ASIC1 pH dependence is changed by exposure to serine proteases (34). The inhibitory toxins and the inactivation-modifying peptides all contain Arg and/or Lys residues that appear to be important for their function (2, 17), while the S18 peptide does not contain Arg or Lys residues. As a caveat, since the experiments were performed with the S18 peptide, we cannot exclude the possibility that other parts of SPLUNC1 might still interact with ASICs.

We found that S18 is able to pull down all three ENaC subunits when they are co-expressed (Figure 5A). However, when each subunit was expressed individually, only the β -ENaC subunit was pulled down (Figure 5B,C). These data suggest that a complex may form between the α , β , and γ ENaC subunits that is pulled down along with β ENaC-S18. Alternatively, it may be possible that when co-expressed, parts of the α and γ ENaC extracellular domains may fold into a different conformation which is conducive to α and γ ENaC binding to S18 when β -ENaC is present.

The predominant band observed in the peptide pull-down assay for β -ENaC, both when all three subunits were co-expressed, and when only the β -ENaC subunit was expressed, was ~94 kDa (Figure 6A, B), which corresponds to glycosylated β -ENaC (25). In contrast, the expected

molecular weight for non-glycosylated β -ENaC is ~73 kDa. When we pulled down β -ENaC and exposed the elution to EndoH, the 94 kDa β -ENaC band pulled down with S18 was shifted to ~73 kDa, indicating that the form of β -ENaC binding to the S18 peptide is glycosylated with non-complex, high mannose *N*-glycans (Figure 6A,B). To confirm this interaction, cells were grown and transfected in the presence of tunicamycin, which prevents *N*-linked glycosylation. Under these conditions, S18 was unable to pull-down the non-glycosylated (i.e. tunicamycin-sensitive) form of β -ENaC (Figure 6C-D). Whilst we cannot exclude the possibility that tunicamycin pretreatment caused mis-folding of the $\alpha\beta\gamma$ ENaC protein, leading to altered S18 binding. taken together, our data lead us to conclude that the S18/ β -ENaC interaction is strongly dependent on the glycosylation state of β -ENaC.

In addition to inhibiting ENaC in oocytes, S18, but not the control peptide ADG, was also capable of reducing ASL absorption and over a period of 24 h, S18 restored ASL height in CF HBECs to ~8 μ m, which is comparable to that observed in normal HBECs (Figures 7A, B). The transepithelial voltage (V_t) was measured in these same cultures to confirm that S18 was in fact functioning by inhibiting ENaC (Figure 7D, E). The thin film V_t reflects a bumetanide -sensitive component (Cl^- secretion through CFTR) and an amiloride/trypsin sensitive component (Na^+ absorption through ENaC) (46). In normal HBECs, the bumetanide-sensitive V_t is stable with time, while the trypsin-sensitive component changes with time as ENaC is inactivated by SPLUNC1 (20, 46). In contrast, in CF HBECs there is no bumetanide-sensitive V_t due to the lack of CFTR and these cultures are also insensitive to trypsin, unless pretreated with a protease inhibitor like aprotinin since ENaC is not spontaneously regulated (46). However, in both normal and CF HBECs, S18 caused a decrease in the 24 h V_t and in CF HBECs, induced trypsin

sensitivity, giving further evidence that S18 is acting through ENaC. Together these data indicate that S18 can serve to restore the regulation of ENaC that is lacking in CF HBECs.

S18 is located at the N-terminus of SPLUNC1 in a region that is intrinsically disordered. Using circular dichroism, we demonstrated that the synthesized S18 peptide also displayed no secondary structure (Figure 8A). This lack of secondary structure was further confirmed by the observation that heat-denatured S18 still prevented ASL hyperabsorption in CF HBECs (Figure 8B). Other investigators have recently shown that unstructured regions of proteins play an important role in protein:protein interactions and that their flexibility is essential to their function (7). It is also possible that the several proline residues followed by a hydrophobic residue in the S18 sequence are important for its function. Proline-rich motifs have been recognized to play an important role in protein:protein interactions (29) and the role of the prolines, as well as the other residues, in S18 are currently being explored to further characterize and optimize its inhibitory function.

Carattino *et al.* previously identified a 26 amino acid peptide that is excised from the α -ENaC subunit during proteolytic processing, residues D206-R231 (14). When these residues are added back to cleaved ENaC they inhibit ENaC activity (14). This 26-mer was further refined to a region of eight amino acids, residues L211-L218 (13). Both the 26-mer and 8-mer α -ENaC peptides caused a reduction in the NP_o of ENaC and they concluded that the reduction largely reflects a change in channel P_o (13, 14, 27). Interestingly, the sequence of the 8-mer, LPHPLQRL, shares 50% sequence identity with residues L24 to T31 (LPVPLDQT) of the S18 peptide. However, the IC₅₀ of the 8-mer was calculated to be 106 μ M and 76 μ M in normal and CF HBECs, respectively, which was much higher than the S18 peptide (0.29 μ M and 0.52 μ M in normal and CF HBECs, respectively). The difference in the IC₅₀s could be due to the

peptide:ENaC subunit interaction and the α -ENaC 8-mer is thought to bind to residues within the finger and thumb domains of α -ENaC (28), while our data show that S18 targets the β -ENaC subunit. Further characterization of the S18 sequence will be needed to distinguish which residues play the largest role in the SPLUNC1 ENaC inhibitory domain.

High levels of proteolytic activity are typically present in the diseased CF lung, leading to potential protein degradation by neutrophil elastase. In the case of S18, this could lead to decreased efficacy and/or duration of action. However, a single dose of S18 prevented CF ASL hyperabsorption over a 24 h period (Figure 7A) and was unaffected by either purified neutrophil elastase or activated neutrophil supernatant (Figure 9A). The ability of S18 to function in a proteolytically active environment makes S18 a strong therapeutic candidate for restoring ASL height in CF patients. Since S18 activity was unaffected by neutrophil elastase, we speculated that a region corresponding to this peptide may be released from SPLUNC1 upon proteolysis. MS analysis revealed that cleavage of recombinant SPLUNC1- Δ 19 by neutrophil elastase indeed resulted in the formation of peptides corresponding to the S18 region (Figure 9C and Table 1), suggesting that release of this region may be a mechanism to make the ENaC inhibitory domain of SPLUNC1 more available during times of inflammation, i.e. when both SPLUNC1 and neutrophil elastase levels are increased. This release of a S18-like region may serve to inhibit ENaC, increase hydration of the mucus layer and increase mucus clearance which would be beneficial for innate lung defense. Interestingly, similar peptides to S18 were observed in normal human sputum samples but were undetectable in CF sputum. While this may suggest that endogenous S18-type peptides are formed in normal ASL, whether they are present at sufficient concentration to regulate ENaC *in vivo* remains to be determined. Free neutrophil elastase is absent from the lungs of healthy individuals. However, the peptides that we detected

may arise from the normal breakdown of SPLUNC1 by the extracellular proteases which are present in the airways (30).

SPLUNC1 is detectable in CF HBEC ASL (21)(Fig. 7B) and may even be upregulated in CF airways, (5, 41). However, we do not detect autoregulation of ENaC in CF HBECs (46). CF airways are moderately acidic due to the lack of bicarbonate secretion through CFTR(16). We have recently demonstrated that SPLUNC1 fails to function in the acidic environment seen in CF ASL due to pH-sensitive conformation changes in SPLUNC1 which reduce SPLUNC1-ENaC interactions (21). This is likely due to pH-sensitive regions on the main SPLUNC1 protein and the S18 peptide alone is pH-independent (21). Consistent with this observation, we found that S18 inhibited Na⁺/ASL absorption in CF HBECs for >24 h following a single dose. This long duration of action may be due to the ability of S18 to bind directly to β-ENaC, unlike the small molecule inhibitor amiloride, which is rapidly transported across the epithelia and has a half-life in the ASL of 10 min (45). Furthermore, we speculate that since S18 binds to β-ENaC, that it will not be actively transported across the airways, and would avoid the off-target effects seen with amiloride and its analogues, such as inhibition of ENaC in the kidneys which can lead to natriuresis and reduced blood pressure. In summary, S18 is heat-stable, protease-resistant and inhibits ENaC/ASL hyperabsorption for up to 24 h in CF HBECs, suggesting that it has therapeutic potential for the treatment of CF lung disease.

References

1. Anantharam A, Tian Y, and Palmer LG. Open probability of the epithelial sodium channel is regulated by intracellular sodium. *J Physiol* 574: 333-347, 2006.
2. Askwith CC, Cheng C, Ikuma M, Benson C, Price MP, and Welsh MJ. Neuropeptide FF and FMRFamide potentiate acid-evoked currents from sensory neurons and proton-gated DEG/ENaC channels. *Neuron* 26: 133-141, 2000.
3. Bartlett JA, Gakhar L, Penterman J, Singh PK, Mallampalli RK, Porter E, and McCray PB, Jr. PLUNC: a multifunctional surfactant of the airways. *Biochem Soc Trans* 39: 1012-1016.
4. Beamer LJ, Carroll SF, and Eisenberg D. The BPI/LBP family of proteins: a structural analysis of conserved regions. *Protein Sci* 7: 906-914, 1998.
5. Bingle L, Barnes FA, Cross SS, Rassl D, Wallace WA, Campos MA, and Bingle CD. Differential epithelial expression of the putative innate immune molecule SPLUNC1 in cystic fibrosis. *Respir Res* 8: 79, 2007.
6. Blanchard MG and Kellenberger S. Effect of a temperature increase in the non-noxious range on proton-evoked ASIC and TRPV1 activity. *Pflugers Arch* 461: 123-139, 2011.
7. Bray D. Flexible peptides and cytoplasmic gels. *Genome Biol* 6: 106, 2005.
8. Bridges RJ. Transepithelial measurements of bicarbonate secretion in Calu-3 cells. *Methods Mol Med* 70: 111-128, 2002.
9. Bruns JB, Carattino MD, Sheng S, Maarouf AB, Weisz OA, Pilewski JM, Hughey RP, and Kleyman TR. Epithelial Na⁺ channels are fully activated by furin- and prostanasin-dependent release of an inhibitory peptide from the gamma-subunit. *J Biol Chem* 282: 6153-6160, 2007.
10. Buchan DW, Ward SM, Lobley AE, Nugent TC, Bryson K, and Jones DT. Protein annotation and modelling servers at University College London. *Nucleic Acids Res* 38: W563-568.
11. Canessa CM, Merillat AM, and Rossier BC. Membrane topology of the epithelial sodium channel in intact cells. *Am J Physiol* 267: C1682-1690, 1994.
12. Canessa CM, Schild L, Buell G, Thorens B, Gautschi I, Horisberger JD, and Rossier BC. Amiloride-sensitive epithelial Na⁺ channel is made of three homologous subunits. *Nature* 367: 463-467, 1994.
13. Carattino MD, Passero CJ, Steren CA, Maarouf AB, Pilewski JM, Myerburg MM, Hughey RP, and Kleyman TR. Defining an inhibitory domain in the alpha-subunit of the epithelial sodium channel. *Am J Physiol Renal Physiol* 294: F47-52, 2008.
14. Carattino MD, Sheng S, Bruns JB, Pilewski JM, Hughey RP, and Kleyman TR. The epithelial Na⁺ channel is inhibited by a peptide derived from proteolytic processing of its alpha subunit. *J Biol Chem* 281: 18901-18907, 2006.
15. Chu HW, Thaikottathil J, Rino JG, Zhang G, Wu Q, Moss T, Refaeli Y, Bowler R, Wenzel SE, Chen Z, Zdunek J, Breed R, Young R, Allaire E, and Martin RJ. Function and regulation of SPLUNC1 protein in Mycoplasma infection and allergic inflammation. *J Immunol* 179: 3995-4002, 2007.
16. Coakley RD, Grubb BR, Paradiso AM, Gatzky JT, Johnson LG, Kreda SM, O'Neal WK, and Boucher RC. Abnormal surface liquid pH regulation by cultured cystic fibrosis bronchial epithelium. *Proc Natl Acad Sci U S A* 100: 16083-16088, 2003.
17. Diochot S, Baron A, Rash LD, Deval E, Escoubas P, Scarzello S, Salinas M, and Lazdunski M. A new sea anemone peptide, APETx2, inhibits ASIC3, a major acid-sensitive channel in sensory neurons. *EMBO J* 23: 1516-1525, 2004.
18. Donaldson SH, Hirsh A, Li DC, Holloway G, Chao J, Boucher RC, and Gabriel SE. Regulation of the epithelial sodium channel by serine proteases in human airways. *J Biol Chem* 277: 8338-8345, 2002.
19. Gally F, Di YP, Smith SK, Minor MN, Liu Y, Bratton DL, Frasch SC, Michels NM, Case SR, and Chu HW. SPLUNC1 promotes lung innate defense against Mycoplasma pneumoniae infection in mice. *Am J Pathol* 178: 2159-2167.

20. **Garcia-Caballero A, Rasmussen JE, Gaillard E, Watson MJ, Olsen JC, Donaldson SH, Stutts MJ, and Tarran R.** SPLUNC1 regulates airway surface liquid volume by protecting ENaC from proteolytic cleavage. *Proc Natl Acad Sci U S A* 106: 11412-11417, 2009.
21. **Garland AL, Walton WG, Coakley RD, Tan CD, Gilmore RC, Hobbs CA, Tripathy A, Clunes LA, Bencharit S, Stutts MJ, Betts L, Redinbo MR, and Tarran R.** Molecular Basis for pH-Dependent Mucosal Dehydration in Cystic Fibrosis Airways. *Proc Natl Acad Sci U S A*, 2013.
22. **Garty H and Palmer LG.** Epithelial sodium channels: function, structure, and regulation. *Physiol Rev* 77: 359-396, 1997.
23. **Haynes J, Jr., Obiako B, Hester RB, Baliga BS, and Stevens T.** Hydroxyurea attenuates activated neutrophil-mediated sickle erythrocyte membrane phosphatidylserine exposure and adhesion to pulmonary vascular endothelium. *Am J Physiol Heart Circ Physiol* 294: H379-385, 2008.
24. **Hobbs CA, Tan CD, and Tarran R.** Does Epithelial Sodium Channel Hyperactivity Contribute to CF Lung Disease? *J Physiol*, 2013.
25. **Hughey RP, Mueller GM, Bruns JB, Kinlough CL, Poland PA, Harkleroad KL, Carattino MD, and Kleyman TR.** Maturation of the epithelial Na⁺ channel involves proteolytic processing of the alpha- and gamma-subunits. *J Biol Chem* 278: 37073-37082, 2003.
26. **Jones DT.** Protein secondary structure prediction based on position-specific scoring matrices. *J Mol Biol* 292: 195-202, 1999.
27. **Kashlan OB, Adelman JL, Okumura S, Blobner BM, Zuzek Z, Hughey RP, Kleyman TR, and Grabe M.** Constraint-based, homology model of the extracellular domain of the epithelial Na⁺ channel alpha subunit reveals a mechanism of channel activation by proteases. *J Biol Chem* 286: 649-660.
28. **Kashlan OB, Boyd CR, Argyropoulos C, Okumura S, Hughey RP, Grabe M, and Kleyman TR.** Allosteric inhibition of the epithelial Na⁺ channel through peptide binding at peripheral finger and thumb domains. *J Biol Chem* 285: 35216-35223.
29. **Kay BK, Williamson MP, and Sudol M.** The importance of being proline: the interaction of proline-rich motifs in signaling proteins with their cognate domains. *FASEB J* 14: 231-241, 2000.
30. **Kesimer M, Kirkham S, Pickles RJ, Henderson AG, Alexis NE, Demaria G, Knight D, Thornton DJ, and Sheehan JK.** Tracheobronchial air-liquid interface cell culture: a model for innate mucosal defense of the upper airways? *Am J Physiol Lung Cell Mol Physiol* 296: L92-L100, 2009.
31. **Kesimer M and Sheehan JK.** Mass spectrometric analysis of mucin core proteins. *Methods Mol Biol* 842: 67-79.
32. **Knowles MR and Boucher RC.** Mucus clearance as a primary innate defense mechanism for mammalian airways. *J Clin Invest* 109: 571-577, 2002.
33. **McGillivray G and Bakaletz LO.** The multifunctional host defense peptide SPLUNC1 is critical for homeostasis of the mammalian upper airway. *PLoS One* 5: e13224.
34. **Poirot O, Vukicevic M, Boesch A, and Kellenberger S.** Selective regulation of acid-sensing ion channel 1 by serine proteases. *J Biol Chem* 279: 38448-38457, 2004.
35. **Randell SH, Fulcher ML, O'Neal W, and Olsen JC.** Primary epithelial cell models for cystic fibrosis research. *Methods Mol Biol* 742: 285-310.
36. **Ratjen F.** Restoring airway surface liquid in cystic fibrosis. *N Engl J Med* 354: 291-293, 2006.
37. **Renard S, Lingueglia E, Voilley N, Lazdunski M, and Barbuy P.** Biochemical analysis of the membrane topology of the amiloride-sensitive Na⁺ channel. *J Biol Chem* 269: 12981-12986, 1994.
38. **Rollins BM, Garcia-Caballero A, Stutts MJ, and Tarran R.** SPLUNC1 expression reduces surface levels of the epithelial sodium channel (ENaC) in Xenopus laevis oocytes. *Channels (Austin)* 4: 255-259.
39. **Rossier BC and Stutts MJ.** Activation of the epithelial sodium channel (ENaC) by serine proteases. *Annu Rev Physiol* 71: 361-379, 2009.
40. **Rowe SM, Miller S, and Sorscher EJ.** Cystic fibrosis. *N Engl J Med* 352: 1992-2001, 2005.
41. **Roxo-Rosa M, da Costa G, Luidor TM, Scholte BJ, Coelho AV, Amaral MD, and Penque D.** Proteomic analysis of nasal cells from cystic fibrosis patients and non-cystic fibrosis control individuals: search for novel biomarkers of cystic fibrosis lung disease. *Proteomics* 6: 2314-2325, 2006.

42. **Sherwood TW and Askwith CC.** Dynorphin opioid peptides enhance acid-sensing ion channel 1a activity and acidosis-induced neuronal death. *J Neurosci* 29: 14371-14380, 2009.
43. **Snyder PM.** Liddle's syndrome mutations disrupt cAMP-mediated translocation of the epithelial Na(+) channel to the cell surface. *J Clin Invest* 105: 45-53, 2000.
44. **Stutts MJ, Canessa CM, Olsen JC, Hamrick M, Cohn JA, Rossier BC, and Boucher RC.** CFTR as a cAMP-dependent regulator of sodium channels. *Science* 269: 847-850, 1995.
45. **Tarran R, Grubb BR, Parsons D, Picher M, Hirsh AJ, Davis CW, and Boucher RC.** The CF salt controversy: in vivo observations and therapeutic approaches. *Mol Cell* 8: 149-158, 2001.
46. **Tarran R, Trout L, Donaldson SH, and Boucher RC.** Soluble mediators, not cilia, determine airway surface liquid volume in normal and cystic fibrosis superficial airway epithelia. *J Gen Physiol* 127: 591-604, 2006.
47. **Voynow JA, Fischer BM, and Zheng S.** Proteases and cystic fibrosis. *Int J Biochem Cell Biol* 40: 1238-1245, 2008.
48. **Yan K, Khoshnoodi J, Ruotsalainen V, and Tryggvason K.** N-linked glycosylation is critical for the plasma membrane localization of nephrin. *J Am Soc Nephrol* 13: 1385-1389, 2002.
49. **Zhou HD, Li XL, Li GY, Zhou M, Liu HY, Yang YX, Deng T, Ma J, and Sheng SR.** Effect of SPLUNC1 protein on the *Pseudomonas aeruginosa* and Epstein-Barr virus. *Mol Cell Biochem* 309: 191-197, 2008.

Acknowledgements

We thank Dr. Rebecca P. Hughey for helpful discussions on the glycosylation experiments. We gratefully acknowledge the technical assistance of Michael Watson, Hong He, and Yan Dang. We also thank the UNC Cystic Fibrosis Center Molecular and Cell Culture Cores, as well as the UNC Macromolecular Interactions Facility.

Grants

Funding was provided by the Cystic Fibrosis Foundation Resource Development Program Grant R026 (CFF RDP-R026), NIH PPG P01 HL034322, 5 P30 DK 065988-08, R01HL103940, R01HL108927 and the UNC-CH School of Medicine.

Disclosures

RT and MJS have founded Spyryx, LLC. The other authors have no financial disclosures.

Author Contributions:

CAH performed S18 pull down assays, all western blots and circular dichroism and co-wrote the paper. CDT performed S18 pull down assays. MG, OA and SK designed and performed experiments regarding ASICS and wrote appropriate sections of the paper. SB provided guidance regarding the structural biology and wrote parts of the paper. RC and MK performed proteomic analysis of SPLUNC1 and wrote sections in the paper. WWG and MR designed and executed SPLUNC1 constructs for purifying Δ19 and Δ44 SPLUNC1 and wrote sections in the paper. AGH obtained sputum samples from normal and CF subjects. MJS measured ENaC currents in *Xenopus* Oocytes and wrote appropriate sections. RT designed experiments, measured ASL height, V_t and co-wrote the paper.

FIGURE LEGENDS

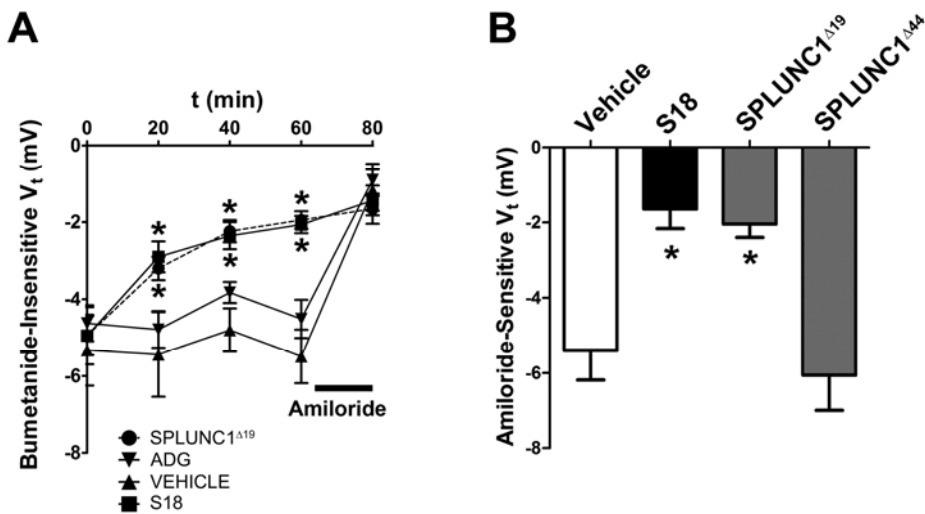


FIGURE 1. Identification of SPLUNC1's ENaC inhibitory domain. A) Normal HBECs were exposed to 100 μ M bumetanide serosally and then V_t was measured immediately before ($t=0$) and at timed intervals after exposure to vehicle (20 μ l Ringer alone), 30 μ M $\Delta 19$ SPLUNC1, S18 or ADG in 20 μ l Ringer. After 60 min, 100 μ M amiloride was added mucosally as a dry powder in perfluorocarbon and V_t was remeasured 20 min later. N.B., amiloride significantly ($p<0.05$) decreased V_t in vehicle and ADG-exposed but not S18- or SPLUNC1 $^{\Delta 19}$ exposed HBECs (statistical symbols omitted for clarity). B) The amiloride-sensitive V_t was measured in normal HBECs after 1 h exposure to vehicle (20 μ l Ringer) or Ringer containing 30 μ M of S18 from SPLUNC1 $^{\Delta 19}$ or SPLUNC1 lacking the S18 region (SPLUNC1 $^{\Delta 44}$). *, $p < 0.05$ different from vehicle.

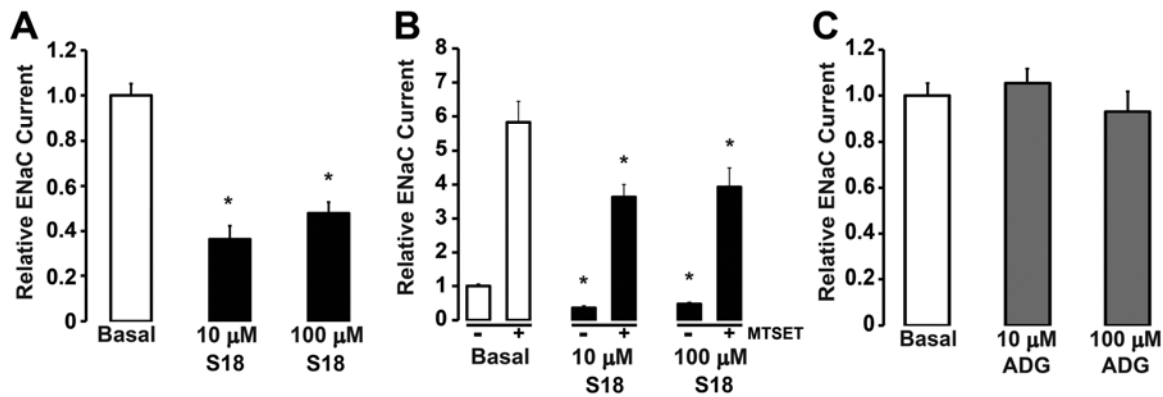


FIGURE 2. S18 inhibits ENaC currents in the *Xenopus* oocyte expression system. A) The effect of 10 and 100 μ M S18 on the amiloride-sensitive ENaC current. B) The effect of MTSET on the amiloride-sensitive ENaC current in the presence or absence of 10 or 100 μ M S18. C) The effect of 10 and 100 μ M ADG on the amiloride-sensitive ENaC current. *, $p < 0.05$ different from vehicle or non-transfected currents as appropriate. † $p < 0.05$ different from S18.

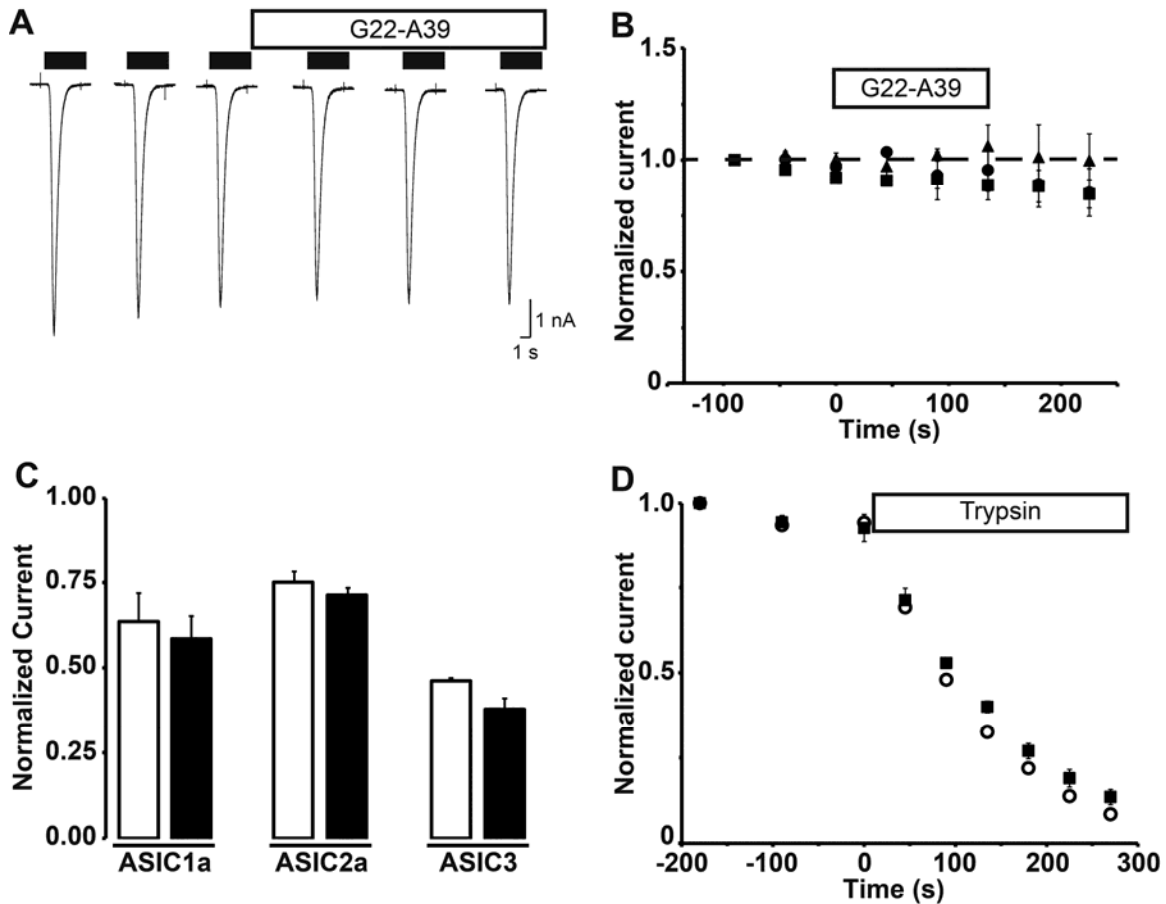


FIGURE 3. Acute S18 peptide exposure does not affect the function of ASIC1a, ASIC2a and ASIC3. Whole-cell currents were measured from CHO cells stably expressing ASIC subunits, voltage clamped to -60 mV. Stimulations lasted 5 s and were performed every 45 s. A) A typical experiment with an ASIC1a-expressing cell is shown. Cells were stimulated three times with pH 6.6 (ASIC1a and -3) or pH 4 (ASIC2a). Between stimulations, cells were returned to a pH 7.4 conditioning solution for 40 s to allow recovery from inactivation. The conditioning solution was then switched to a pH 7.4 solution containing 10 μ M S18. Three stimulations in the presence of 10 μ M S18 were performed before washing off the peptide. B) Current amplitudes of the above described experiments were normalized to the first control value and plotted as a function of time. S18 was added at T = 0 s. ASIC1a = ■, ASIC2a = ●, ASIC3 = ▲, all n = 3. C) Cells were incubated for 40 s in a pH 7.1 (ASIC1a and -3) or 5.6 (ASIC2a) conditioning solution, then activated using an acidic stimulus (pH 5 for ASIC1a and -3, and pH 4 for ASIC2a). Experiments were performed with or without 10 μ M S18 in the conditioning solution. Current amplitudes measured during the acidic stimulus were normalized to the control amplitude obtained with a pH 7.4 conditioning solution. Open bars = control, closed bars = S18, all n = 3-4. D) Cells expressing ASIC1a were stimulated three times with a pH 6.6 stimulus before 40 μ g/ml trypsin was added to the pH 7.4 solution. Stimulations were performed every 45 s. The protocol was performed with or without 10 μ M S18 in all solutions. The average current is plotted as a function of time. Trypsin was added at T = 0 s. Control = ○, S18 = ■, all n = 3-5.

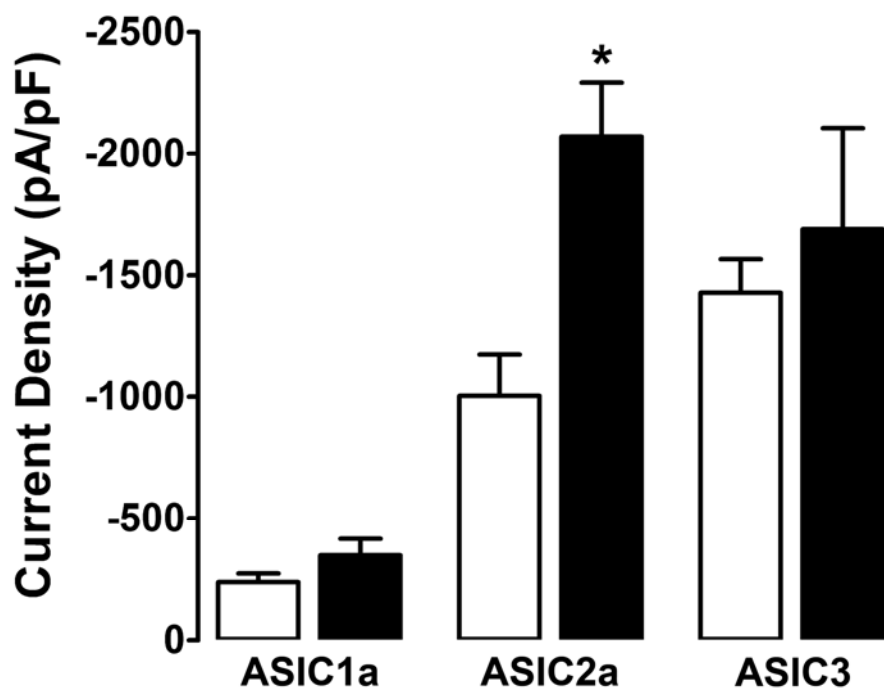


FIGURE 4. 1 h S18 peptide exposure stimulates ASIC2a. CHO cells stably expressing ASIC subunits were exposed to vehicle (Ringer, open bars) or S18 (10 μ M, closed bars) for 1 h. Voltage was clamped to -60 mV and whole-cell currents were measured. ASIC1a, n=7. ASIC2a, n=9, ASIC3, n=9. *, $p < 0.05$ different from vehicle.

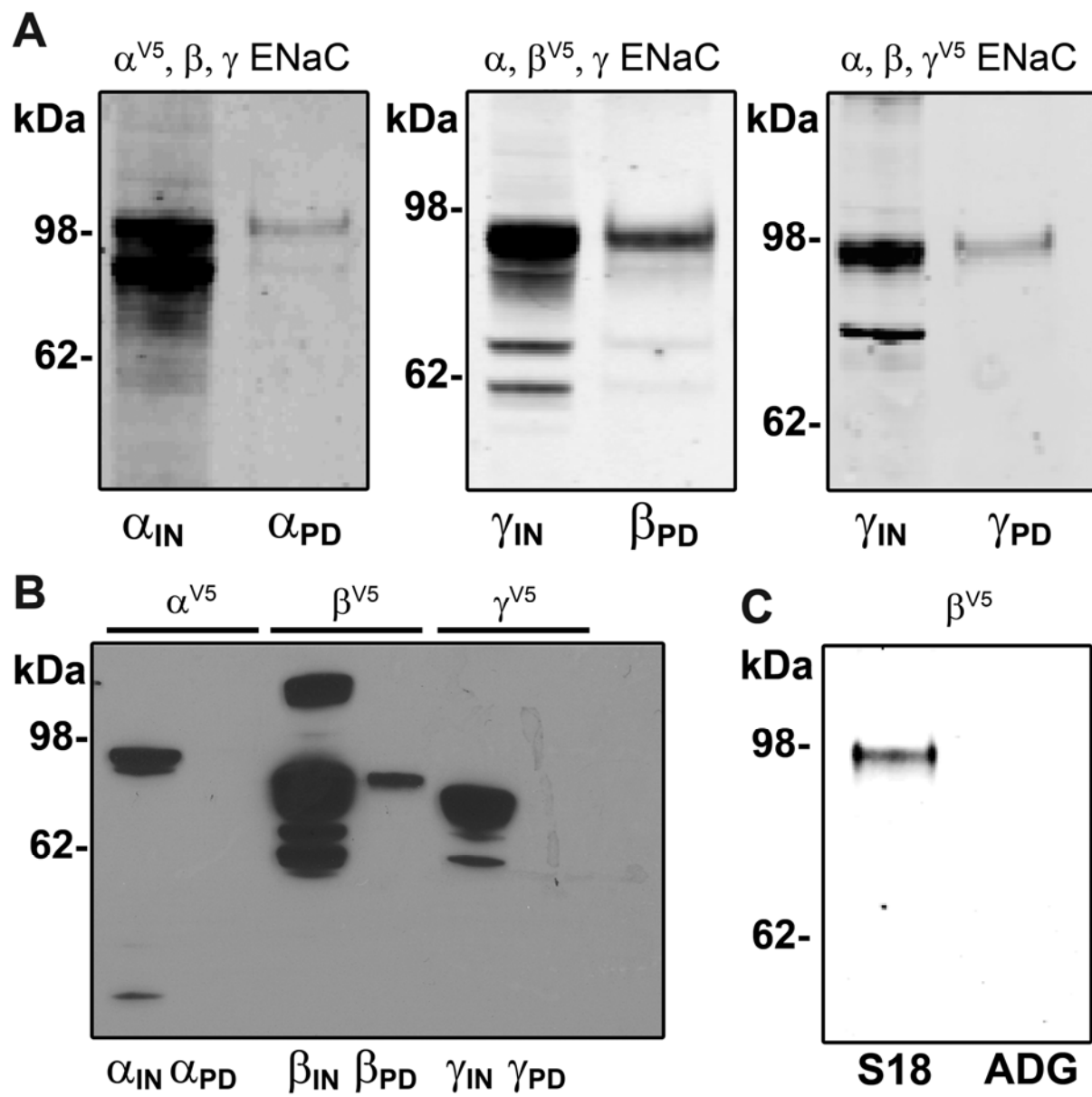


FIGURE 5. Analysis of S18-ENaC Interactions. A) Typical western blot of the triple-transfected $\alpha\beta\gamma$ -ENaC peptide pull-down assay. The pull-down assay was performed with one V5-tagged subunit and two untagged subunits as designated. B) Typical western blot of the S18 peptide pull-down assay of individually expressed ENaC subunits. IN = input, PD = pull-down elution. C) Typical western blot showing the pull-down assay performed with S18 or ADG. No β -ENaC was observed in the elution with the ADG peptide confirming that the observed β -ENaC is from specific interaction with the S18, n = 3.

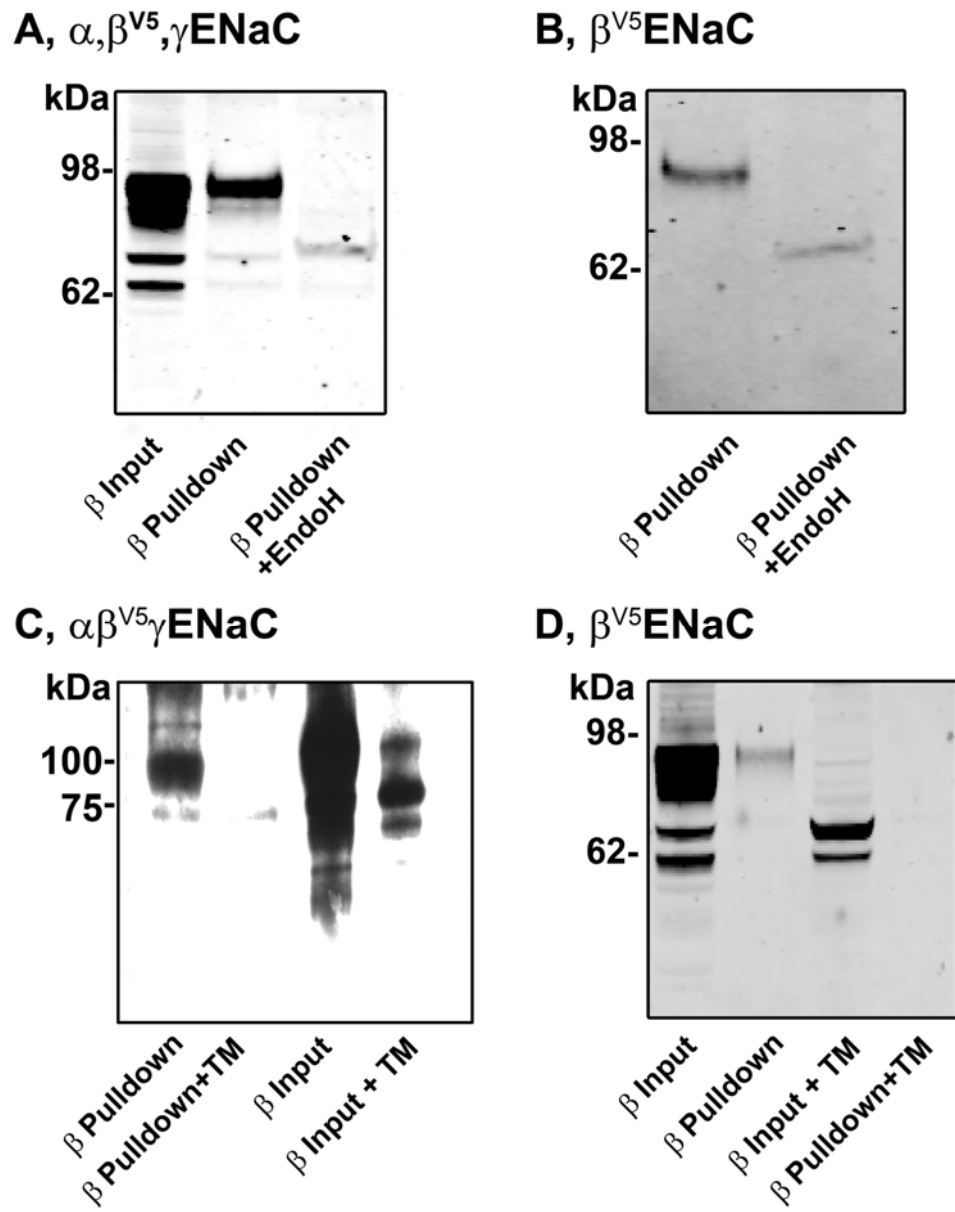


FIGURE 6. The β -ENaC/S18 interaction is glycosylation dependent in HEK293T cells. A) Typical western blot of the $\alpha\beta\gamma$ -ENaC peptide pull-down assay with the β -ENaC subunit V5-tagged and untagged α and γ -ENaC subunits. The pull-down assay was performed and the elution treated with EndoH. B) Typical western blot of the β -ENaC only peptide pull-down assay with the β -ENaC subunit V5-tagged. The pull-down assay was performed and the elution treated with EndoH. C) Typical western blot of the tunicamycin pre-treated β -ENaC pull-down assay when cells were co-transfected with V5-tagged β -ENaC and untagged α and γ -ENaC subunits. D) Typical blot of the tunicamycin pre-treated β -ENaC pull-down assay when cells were transfected with V5-tagged β -ENaC alone. All n = 3.

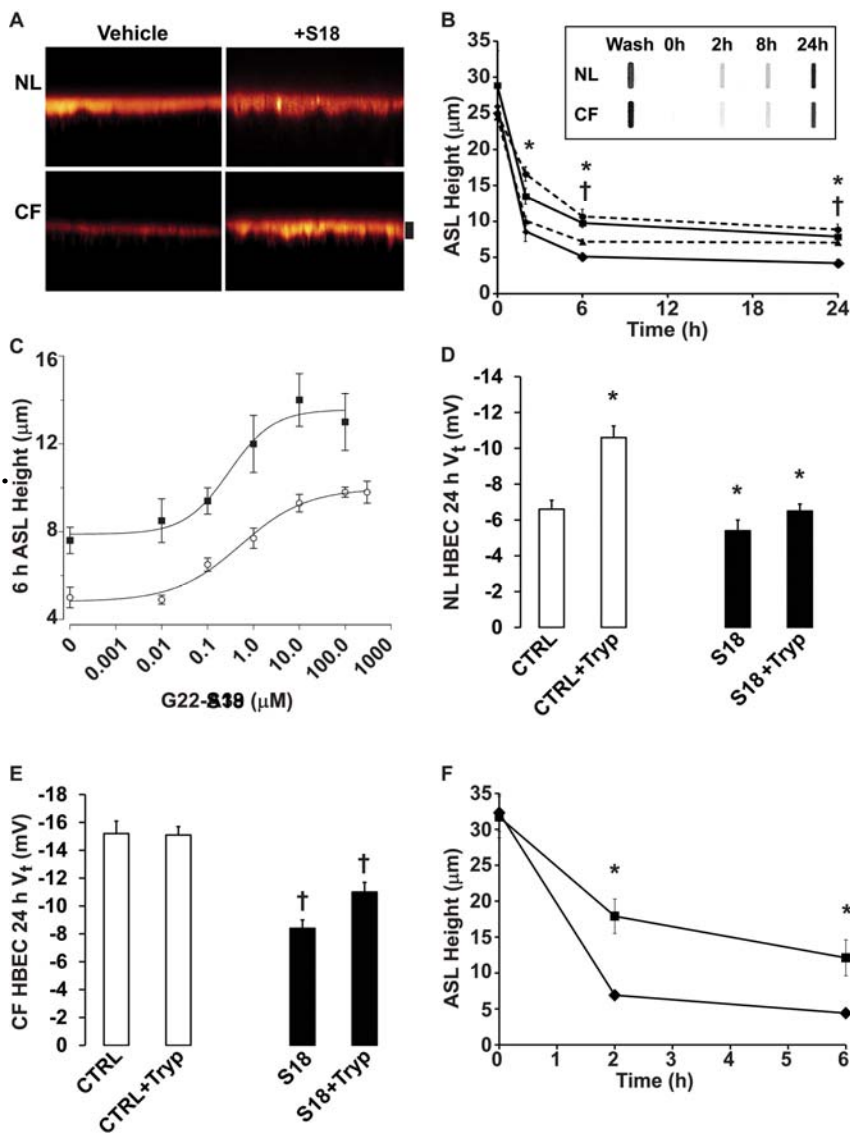


FIGURE 7. S18 inhibits CF ASL hyperabsorption. A) Confocal micrographs of normal and CF ASL height 24 h after exposure to S18 or vehicle (control). Scale bar = 7 μm . B) Mean ASL height over time in normal and CF HBECs with or without addition of S18; dashed lines are normal HBECs (ctrl = \blacktriangle , S18 = \bullet), non-dashed lines are CF HBECs (ctrl = \blacklozenge , S18 = \blacksquare), n = 6; *, p < 0.05 different from basal. Inset: Typical slot blot for SPLUNC1 lavaged from the mucosal surfaces of normal and CF HBECs at timed intervals. Mucosal surfaces were left undisturbed for 24 h, washed immediately prior to initiating ASL height experiments, and in parallel cultures, subsequent SPLUNC1 recovery was determined. C) Change in ASL height with increasing concentration of S18 in normal (closed) and CF (open) HBECs. D) Thin film transepithelial PD for normal HBECs. Open bars = control, closed bars = S18, n = 10. E) Thin film transepithelial PD for CF HBECs. Open bars = control, closed bars = S18, n = 6. F) ASL height over time in normal HBECs in the presence of 100 μM bumetanide with (■) or without S18 (◆), n = 6. * = normal p < 0.05 different ± S18 or ± trypsin. † = CF p < 0.05 different ± S18.

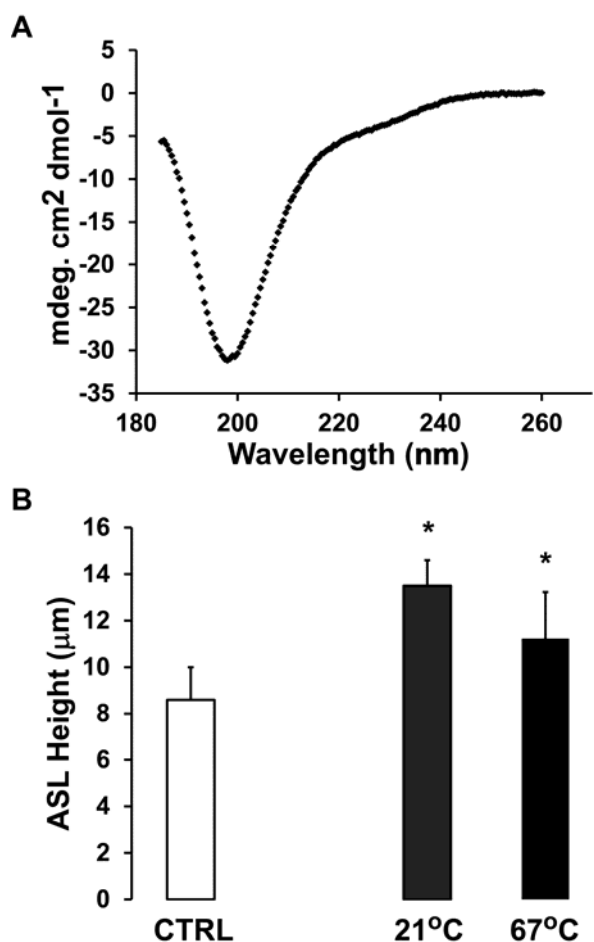


FIGURE 8. S18 maintains ASL height of CF HBECs with no intrinsic structure. A) Far-UV CD spectra of S18 at 25°C. B) ASL height of CF HBECs at 2 h. Control = open bar, S18 at 21°C = gray bar, S18 heated to 67°C then added to the culture = black bar.

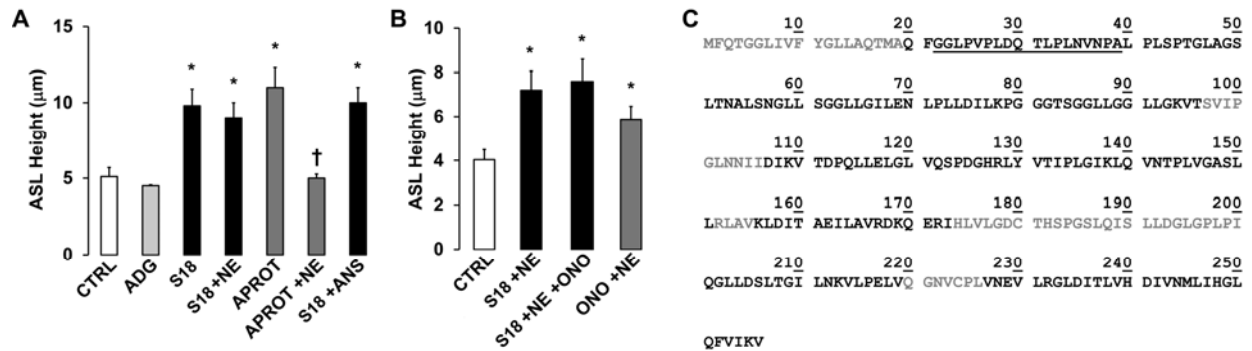


FIGURE 9. S18 prevents ASL hyperabsorption in the presence of neutrophil elastase. A, B, Bargraphs of ASL height at 8 h in CF HBECs. A) Control (open bar), 100 μM S18 (black bars), and 10 μM aprotinin (gray bars). NE = neutrophil elastase, APROT = aprotinin, ANS = activated neutrophil supernatant. NE was added at 100 nM. ANS was diluted 1:1 with PBS. All n = 6. * $p < 0.05$ different to control. † $p < 0.05$ different to aprotinin. B) Bargraph of ASL height in CF HBECs at 8 h. Control (open bar), 100 μM S18 with 100 nM NE with or without ONO (black bars), and 10 μM ONO (gray bar). All n = 6. * $p < 0.05$ different to control. C) Sequence of SPLUNC1 obtained by mass spectrometry with the observed residues after 5 min exposure to neutrophil elastase in black. The S18 peptide is underlined.

TABLE 1. Peptides observed by mass spectrometry in the neutrophil elastase 5-min cleavage assay of Δ19-SPLUNC1-

Residue	Sequence	Residue	Sequence
23-45	GLPVPLDQTLPLNVNPALPLSPT	122-131	QSPDGHRLYV
27-45	PLDQTLPLNVNPALPLSPT	123-131	SPDGHRLYV
32-45	LPLNVNPALPLSPT	124-131	PDGHRLYV
46-61	GLAGSLTNALSNGLLS	125-131	DGHRLYV
46-67	GLAGSLTNALSNGLSSGGLGI	132-141	TIPLGIKLQV
46-86	GLAGSLTNALSNGLSSGGLGILENLPLLDILKPGGGTSGGG	132-148	TIPLGIKLQVNTPLVGA
53-86	NALSNGLSSGGLGILENLPLLDILKPGGGTSGGG	132-155	TIPLGIKLQVNTPLVGASLLR
53-95	NALSNGLSSGGLGILENLPLLDILKPGGGTSGGLGGLLGKV	138-148	KLQVNTPLVGA
53-96	NALSNGLSSGGLGILENLPLLDILKPGGGTSGGLGGLLGKV	138-149	KLQVNTPLVGAS
54-95	ALSNGLSSGGLGILENLPLLDILKPGGGTSGGLGGLLGKV	138-151	KLQVNTPLVGASLL
62-95	GGLLGILENLPLLDILKPGGGTSGGLGGLLGKV	142-155	NTPLVGASLLR
62-96	GGLLGILENLPLLDILKPGGGTSGGLGGLLGKV	149-155	SLLR
67-95	IENLPLLDILKPGGGTSGGLGGLLGKV	156-166	KLDITAEILAV
68-95	LENLPLLDILKPGGGTSGGLGGLLGKV	156-173	KLDITAEILAVRDKQERI
74-86	LDILKPGGGTSGG	160-173	TAEILAVRDKQERI
77-95	LKPGGGTSGGLGGLLGKV	164-173	LAVRDKQERI
77-96	LKPGGGTSGGLGGLLGKV	165-172	AVRDKQER
84-95	SGGLGGLLGKV	165-173	AVRDKQERI
84-96	SGGLGGLLGKV	166-173	VRDKQERI
87-95	LLGGLLGKV	201-219	QGLLDSLTGILNKVLPELV
87-96	LLGGLLGKV	231-236	LRGLDI
106-131	DIKVTDQPQLLELGLVQSPDGHRLYV	231-239	LRGLDITLV
107-118	DIKVTDQPQLEL	231-243	LRGLDITLVHDIV
107-121	DIKVTDQPQLLELGLV	231-247	LRGLDITLVHDIVNMLI
107-131	DIKVTDQPQLLELGLVQSPDGHRLYV	237-247	TLVHDIVNMLI
109-118	KVTDPQLEL	240-247	HDIVNMLI
109-121	KVTDPQLELGLV	240-256	HDIVNMLIHLQFVIKV
109-131	KVTDPQLELGLVQSPDGHRLYV	248-253	HGLQFV
111-131	TDPQLELGLVQSPDGHRLYV	248-254	HGLQFVI
119-131	GLVQSPDGHRLYV	248-256	HGLQFVIKV
121-131	VQSPDGHRLYV		